A numerical experiment on the influence of the interannual variation of sea surface temperature on terrestrial precipitation in northern Japan during the cold season

Tomonori Sato[1] and Shiori Sugimoto[1]

Received 30 October 2012; revised 1 November 2013; accepted 2 November 2013; published 26 November 2013.

[1] The role of sea surface temperature (SST) anomaly in modulating the terrestrial precipitation in winter around Japan was investigated using a regional atmospheric model. Large amount of snowfall occurs as the westerly winter monsoon carries abundant moisture from the Japan Sea. An experiment with realistic SST gives improved representation of terrestrial precipitation distribution compared to the reanalysis. The standard deviation of interannual variation of precipitation in the experiment was approximately 20% larger over the Kuroshio extension than that in the experiment with climatology SST, suggesting that the SST variability enhances the oceanic precipitation variability. For the role of Japan Sea, the terrestrial precipitation over the Japan Sea side (JSS) region in northern Japan was sensitive to the offshore SST anomaly through affecting moisture flux toward Japan. Since the offshore SST was clearly warmer in the 2000s relative to the 1980s, the effect of the long-term SST variation on the terrestrial precipitation trend was examined. The experiment with realistic SST simulated the observed trend in terrestrial precipitation in the JSS region. In contrast, the precipitation trend was significantly reduced in the experiment with climatology SST. Therefore, the long-term SST trend is an important factor for the precipitation trend in the region of Japan and the adjacent oceans where SST has significant trends. Precipitation in southern Japan facing the Pacific Ocean indicated increasing trend even without the SST trend. This suggests that the long-term variations in extratropical cyclones are also an important factor for precipitation trends around the Kuroshio extension.

Citation: Sato, T., and S. Sugimoto (2013), A numerical experiment on the influence of the interannual variation of sea surface temperature on terrestrial precipitation in northern Japan during the cold season, *Water Resour. Res.*, *49*, 7763–7777, doi:10.1002/2012WR013206.

1. Introduction

[2] The interaction between the ocean and atmosphere regulates the mean state and variability of the earth's climate in various time scales through heat, moisture, and carbon exchanges. The large heat capacity of the ocean makes the seasonal variation of sea surface temperature (SST) smoother compared to that of the land surface temperature. During the cold season, land masses cool more strongly than the ocean, resulting in a strong surface pressure gradient between the continents and adjacent oceans. In particular, the Siberian high, which develops over the eastern part of the Eurasian continent, consists of coldest dry air mass and brings cold outbreaks toward the East Asian region [*Wang*, 2006].

[3] The northern part of Japan facing the Japan Sea (Figure 1) receives a lot of snowfall in the cold season (Figure 2). Figure 2a illustrates the climatology pattern of sea level pressure in December-January-February during the winter of 1982/1983 to that of 2007/2008 using the Japanese 25 year reanalysis (JRA-25) [*Onogi et al*., 2007]. The pressure gradient between the Eurasian Continent and Northwestern Pacific is the driving force of the winter monsoon. The heavy precipitation in north Japan is caused as a result of interaction between winter monsoon and Japan Sea as proposed in earlier studies [e.g., *Manabe*, 1957; *Ninomiya*, 1968]. As the continental air mass proceeds eastward over the Japan Sea, the vertical temperature profile becomes absolutely unstable in the lower layer because of heat and moisture supplied from the warm ocean, which causes rapid air-mass transformation over the Japan Sea [*Manabe*, 1957; *Ding*, 1994]. After the transformation, the air mass contains abundant moisture. The northwesterly wind due to the winter monsoon is forced to ascend along the mountain range of central Japan, causing heavy precipitation in the Japan Sea side (JSS) region over terrestrial Japan [e.g., *Saito et al*., 1996] (see Figures 1 and 2). The snowpack begins to disappear in spring, and the melted water is widely used for human activities, such as agriculture. The winter precipitation in this region is, therefore, an important water resource for the local population.

[4] The interannual variability of winter monsoon plays a leading role in the interannual variation of the snowfall in JSS regions. Figure 2b displays the relationship between

[1]Faculty of Environmental Earth Science, Hokkaido University, Sapporo, Japan.

Corresponding author: T. Sato, Faculty of Environmental Earth Science, Hokkaido University, Kita-10, Nishi-5, Sapporo 060–0810, Japan. (t_sato@ees.hokudai.ac.jp)

0043-1397/13/10.1002/2012WR013206

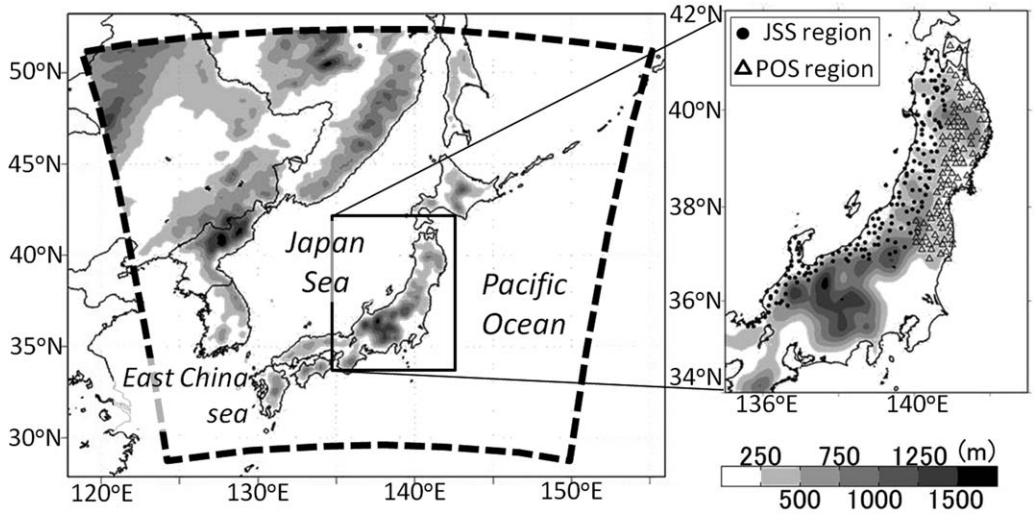

Figure 1. Topography (m) around the studied area. Dots and triangles indicate locations of meteorological station in JSS (Japan Sea side) and POS (Pacific Ocean side) regions divided by the mountain ridge, respectively. Both regions represent only land areas. Broken line indicates the model domain.

the interannual variation of maximum snow depth in JSS region and the winter monsoon. The monsoon index has been traditionally used to represent the pressure gradient between Eurasian continent and North Japan [e.g., *Yasuda and Hanawa*, 1999; *Hirose and Fukudome*, 2006] and is defined by the sea level pressure difference between Irkutsk

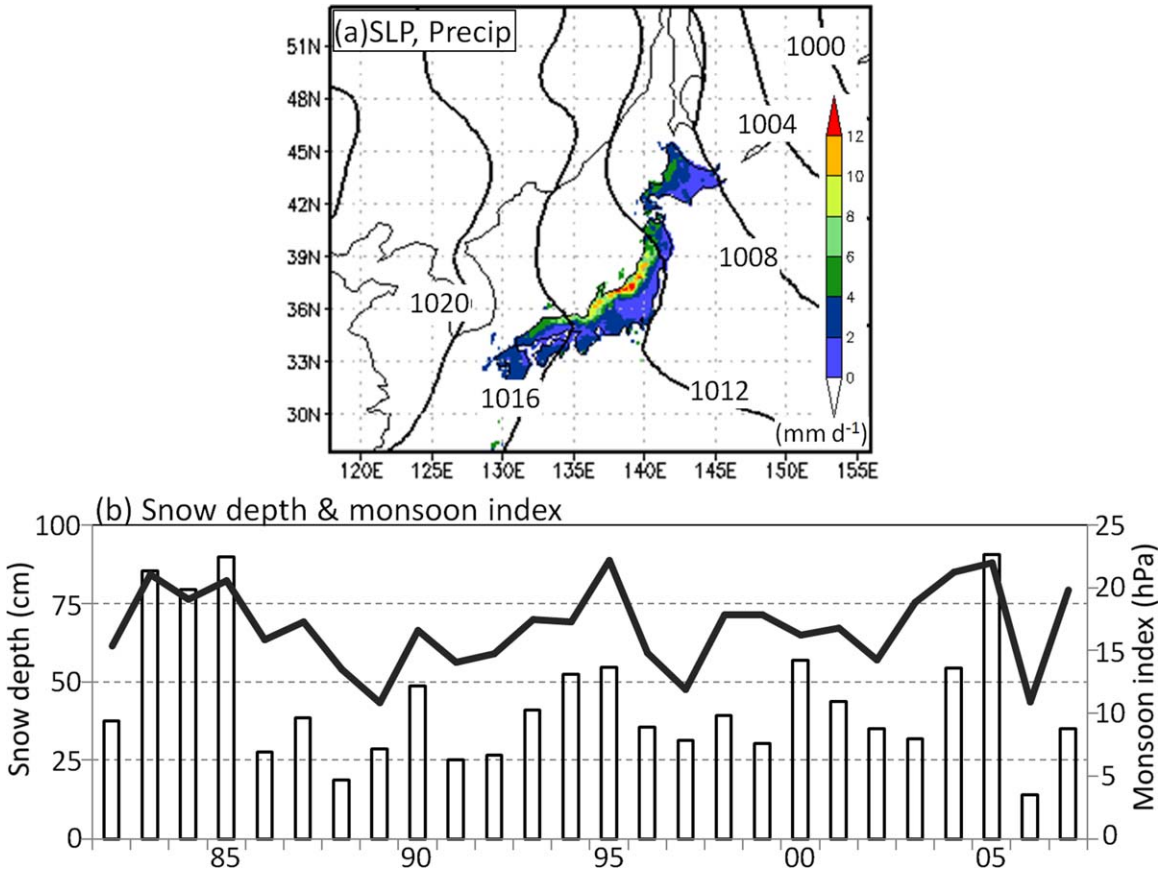

Figure 2. (a) December-January-February mean sea level pressure (contour: hPa) and precipitation (mm day^{-1}) in Japan. (b) Interannual variations of snow depth (cm; bar) in JSS region (Figure 1) and the monsoon index (line). The sea level pressure and monsoon index are computed by using JRA-25 reanalysis, and snow depth is derived from surface observations. The precipitation data are obtained from the APHRODITE data set [*Kamiguchi et al*., 2010].

(52.5°N, 103.75°E) and Nemuro (43.75°N, 145.0°E). A high correlation between the monsoon index and snow depth in JSS region ($R = 0.745$) suggests that the atmospheric variability is a crucial factor for the snow depth variability. Meanwhile, considering the air mass transformation process over the Japan Sea, the ocean's role in modulating winter precipitation in Japan should be also important. However, it is difficult to answer the question of how and how strong does SST affect the interannual variation and long-term trends in winter precipitation around Japan.

[5] The Japan Sea is a semienclosed sea surrounded by land masses. The winter SST variation in the Japan Sea is roughly explained by the three components: air-sea heat exchange, heat supply from the warm Tsushima current that passes through the Korea/Tsushima Strait between the Japanese islands and the Korean Peninsula, and the cold Liman current. Figure 3 illustrates the monthly mean SST distribution averaged from the winter of 1982/1983 to that of 2007/2008 using the Optimum Interpolation SST (OISST) data set [*Reynolds et al*., 2007]. SST is high from the central to eastern parts of the Japan Sea because of the presence of a warm ocean current. A low SST region extends from the western to central part of the Japan Sea during December–March, suggesting intense cooling of the ocean surface because of the cold winter monsoon from the Eurasian continent and the Liman current. The standard deviation of the interannual variation of SST is large during December–February around the central Japan Sea, reflecting the interannual variation of the winter monsoon and ocean structures. The mean SST distribution in the Western North Pacific exhibits a strong meridional gradient near the eastern coast of the Japanese islands corresponding to the Kuroshio extension where high standard deviation is also evident. In December and January, the magnitude of the interannual variation of SST is similar in the Japan Sea and the Pacific Ocean or slightly larger in the Pacific Ocean, whereas in March and April, the magnitude of the interannual variation of SST in the Pacific Ocean is considerably larger than that in the Japan Sea. Since the magnitude of the interannual variation of SST differs significantly depending on the season and the location, it is interesting to investigate the impact of SST variability on winter precipitation around Japan. Recent studies have suggested a possible influence of the SST anomalies around Japan on the atmospheric circulation [e.g., *Tokinaga et al*., 2006; *Taguchi et al*., 2009; *Koseki and Watanabe*, 2010; *Iizuka*, 2010; *Xu et al*. 2011]. *Taguchi et al*. [2009] investigated the storm track activity that is affected by the air-sea interaction during the winter of 2003/2004. *Koseki and Watanabe* [2010] performed a general circulation model (GCM) simulation to investigate the effect of mesoscale SST distribution on the atmospheric boundary layer over the Kuroshio extension. Despite the considerable efforts using the climate models, their experimental setting was insufficient to examine terrestrial precipitation in Japan mainly because of the low resolution of the models.

[6] Regional climate models generally have a higher resolution than the GCMs; this enabled investigations of the effects of high-resolution SST data on mesoscale atmospheric structures [e.g., *Iizuka*, 2010; *Xu et al*., 2011]. The results of these studies suggest that mesoscale SST distribution alters surface sensible and latent heat fluxes, eventually causing a change in atmospheric convective processes. However, no study has adequately addressed the possible influence of spatial and temporal SST variability on the terrestrial precipitation variability in this area. Therefore, this study aims at investigating the influence of SST's variability and long-term trend on the winter precipitation in Japanese Island by using a regional atmospheric model. *Hong and Yhang* [2010] showed that the regional climate model has limited capability for simulating the decadal shift in precipitation over East Asia. This study will demonstrate the attribution of recent precipitation trend in Japan by a pair of long-term experiment using a regional model.

[7] In this paper, the regional model setup is explained in section 2. The model performance for simulating the observed precipitation and snow is presented in section 3 followed by the results on the influence of SST on precipitation variability around Japan. The relationship between long-term SST and precipitation variations is shown in section 4. In section 5, we discuss the role of SST in the Pacific Ocean. section 6 presents the conclusion.

2. Model and Experimental Setup

[8] To elucidate the effect of the interannual variation of SST in modulating winter precipitation around Japan, long-term numerical experiments were conducted using the Weather Research and Forecasting (WRF) model version 3.2.1 with the Advanced Research WRF dynamical core [*Skamarock et al*., 2008]. The model domain was centered on the Japanese Islands which includes the entire Japan Sea to simulate the transformation of the continental air mass over the ocean (Figure 1). To conduct a couple of numerical experiments in this domain over a long period, the horizontal mesh size was set to 20 km (130 × 130 grid). The mesh size of 20 km is not very high in comparison to the earlier studies [e.g., *Hara et al*., 2008; *Gutmann et al*., 2012]; but it is sufficient to capture seasonal and interannual variations of precipitation and snow depth in Japan (see section 3). The vertical grid has 32 layers. The physics parameterizations adopted were the cumulus convection scheme [*Grell and Devenyi*, 2002], cloud microphysics scheme [*Hong et al*., 2004; *Hong and Lim*, 2006], shortwave radiation scheme [*Dudhia*, 1989], long-wave radiation scheme [rapid radiative transfer model; *Mlawer et al*., 1997], planetary boundary layer scheme [*Nakanishi and Niino*, 2004, 2006], and Noah land surface model [*Chen and Dudhia*, 2001]. The cloud microphysics scheme adopts six categories of hydrometeors which allows representing mixed-phase processes as well as ice-phase processes. The Noah land surface model predicts the accumulation and melting of the surface snow cover. The snow cover is expressed as a single layer in which temporal variations of snow water equivalent, snow depth, and surface albedo are simulated. The snow depth is determined as a result of sublimation and melting at the top and bottom surfaces of the snowpack which are computed in the land surface model by using variables from the atmospheric model (such as radiation, temperature, and precipitation) as the inputs. The WRF was driven using an atmospheric forcing data set obtained from the JRA-25 on 1.25° grid. The four outermost rows of the grid points from the lateral boundary were

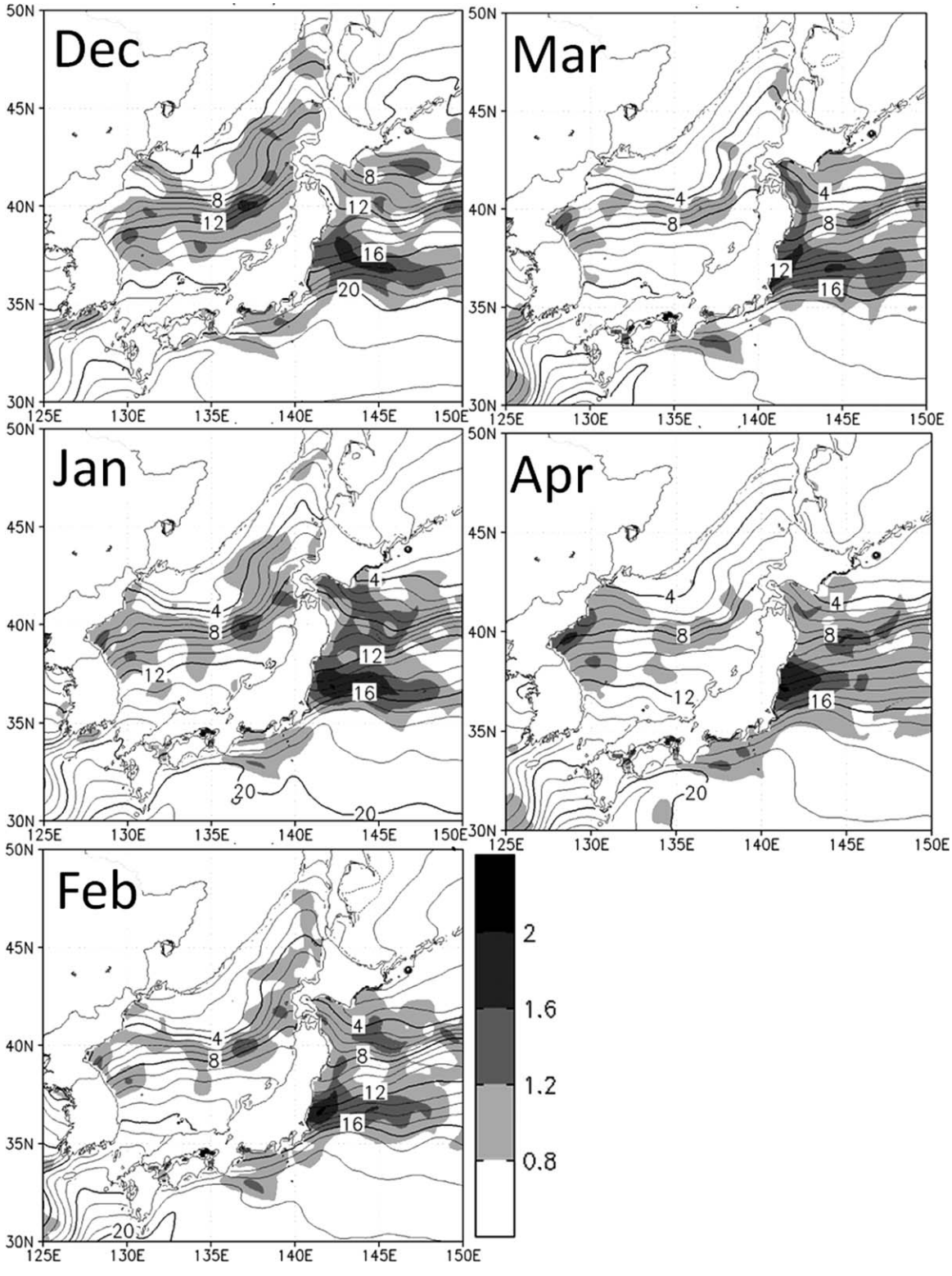

Figure 3. Monthly mean sea surface temperatures (°C) during 1982/1983 winter to 2007/2008 winter (contour) and their standard deviations for interannual variation (shade).

nudged to the forcing data set. The daily mean SST [OISST; *Reynolds et al*., 2007] on 0.25° mesh grid was used as the ocean surface boundary condition since it has similar horizontal resolution with the atmospheric model. The period of simulation was 26 years from the winter of 1982/1983 to that of 2007/2008. The starting date for each year's numerical integration was 15 October and the ending date was 30 April of the following year, covering the snowy season in Japan. The first 45 days were for spin-up intended to include the beginning of the snow accumulation

over the mountain area. The latter 5 months, i.e., from December to April, were applied for the analysis. Hereafter, the numerical experiments with the aforementioned setting are referred to as the REAL runs.

[9] To verify the effect of the interannual variation of SST, a sensitivity experiment was conducted. In the REAL runs, the daily mean SST data set obtained from OISST was used as the surface boundary condition. For the sensitivity experiment, the 26 year mean daily climatology SST was computed using OISST, and then applied to all 26 years; thus, eliminating the interannual variation of SST (hereinafter, referred to as CLIM runs). The difference between the REAL and CLIM runs provided the atmospheric response derived only from the SST variability, such as the interannual variation of SST and long-term SST trends. The 26 year long simulation is advantageous in the following regards. Because of interannual variations in the real atmosphere and ocean systems, the atmospheric response to the surface forcing will appear in different ways during different years [e.g., *Sato and Xue*, 2013]. For example, the effect of the high SST anomaly for modulating terrestrial precipitation may be smaller in a weak winter monsoon year than that in a strong winter monsoon year because the air-mass transformation is related to the temperature difference between the atmosphere and ocean. A multiyear sensitivity simulation enables us to investigate the robustness of the atmospheric response to the SST forcing under various atmospheric conditions.

3. Results

3.1. Verification of the Simulated Climate

[10] A climatology mean pressure pattern in the REAL runs is illustrated in Figure 4. The sea level pressure indicates west-high east-low pattern that is very similar to the reanalysis (Figure 2a). Although the pressure contour lines shows a complex pattern over the Eurasia because of the high resolution topography, the WRF well captures the mean pressure gradient that is necessary to force the winter monsoon. The simulated precipitation in Japan is also very similar to that observed (Figure 2a) which shows high precipitation along the area facing to the Japan Sea.

[11] Figure 5 depicts the 26 year mean seasonal variation of snow depth and precipitation in the JSS and Pacific Ocean side (POS) regions (see Figure 1). The boundary between two regions corresponds to the major mountain ridge. The outputs of REAL runs are linearly interpolated to obtain the point values corresponding to the JMA's observation sites. The seasonal variation of snow depth in the JSS and POS regions reached a maximum in February, the coldest period, with more than 70 cm in the JSS region. WRF successfully simulated the amount and seasonal variation of snow depth in the two regions (Figures 5a and 5b). The simulated precipitation also captured the seasonal variation and regional differences well. However, WRF tended to overestimate the precipitation during January–March in the JSS region and during December–March in the POS region. *Yamaguchi et al*. [2009] reported that gauge-based measurements tend to underestimate the winter precipitation because of their low collection efficiency for snowflakes; hence, the amount of actual precipitation would be larger than the observed value shown in Figure 5. The

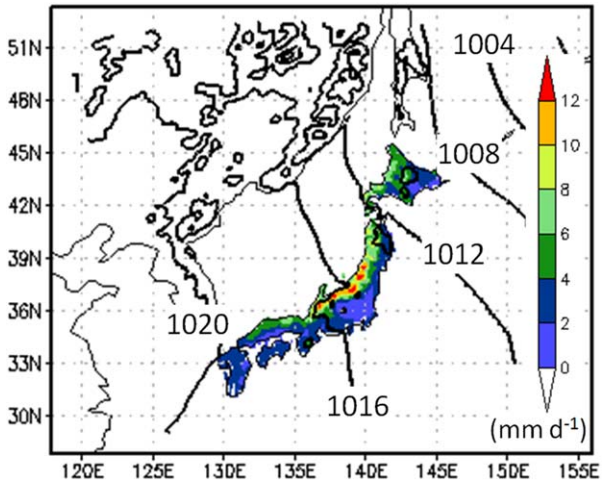

Figure 4. December-January-February mean sea level pressure (contour: hPa) and precipitation in Japan (shade: mm day^{-1}) in REAL runs.

monthly mean temperature in the REAL runs was compared with the JMA's observations. The WRF produced a temperature variation similar to that observed in JSS and POS regions. The simulated temperature is, however, obviously lower than the observation by 1–3 K.

[12] The WRF successfully produced the observed interannual variation of mean snow depth in the JSS region (Figure 6a). The correlation for the interannual variation was 0.97. The snow depth was large during the winters of 1983/1984–1985/1986 and 2005/2006. Unlike its good performance for snow depth, WRF overestimated the mean precipitation with a mean bias of 27.2 mm month^{-1} (Figure 6b). The WRF's precipitation results roughly follow the observed interannual variation ($R = 0.77$) including years with high precipitation, such as 1990/1991, and less precipitation, such as the winter of 2002/2003. The bias of snow depth in the WRF experiment is partly due to the model, i.e., sensitivity of snowfall to the choice of microphysics scheme, and also to the observation errors which relates to collection rate, sublimation, and wind-induced redistribution of snow. The correlation for precipitation was 0.55 in the CLIM run, suggesting the importance of SST's interannual variation for simulating the realistic interannual variation of precipitation as well as the atmospheric variability (i.e., lateral boundary forcing).

[13] The Taylor diagram [*Taylor*, 2001] for monthly mean precipitation is shown in Figure 7. The Taylor diagram is used to investigate the difference of the model results relative to the reference data by showing spatial correlation and standard deviation. Here, the APHRODITE data were used as a reference data which is a gridded daily precipitation data set that consists mainly of the JMA's rain gauge observations [*Kamiguchi et al*., 2010]. The angle from the lateral axis indicates the pattern correlation, and the radius from the origin (0, 0) indicates the standard deviation against the observed precipitation. The distance from the reference (APHRODITE's observation, star) corresponds to the root-mean-squared error (RMSE). The simulated precipitation climatology over Japan is much

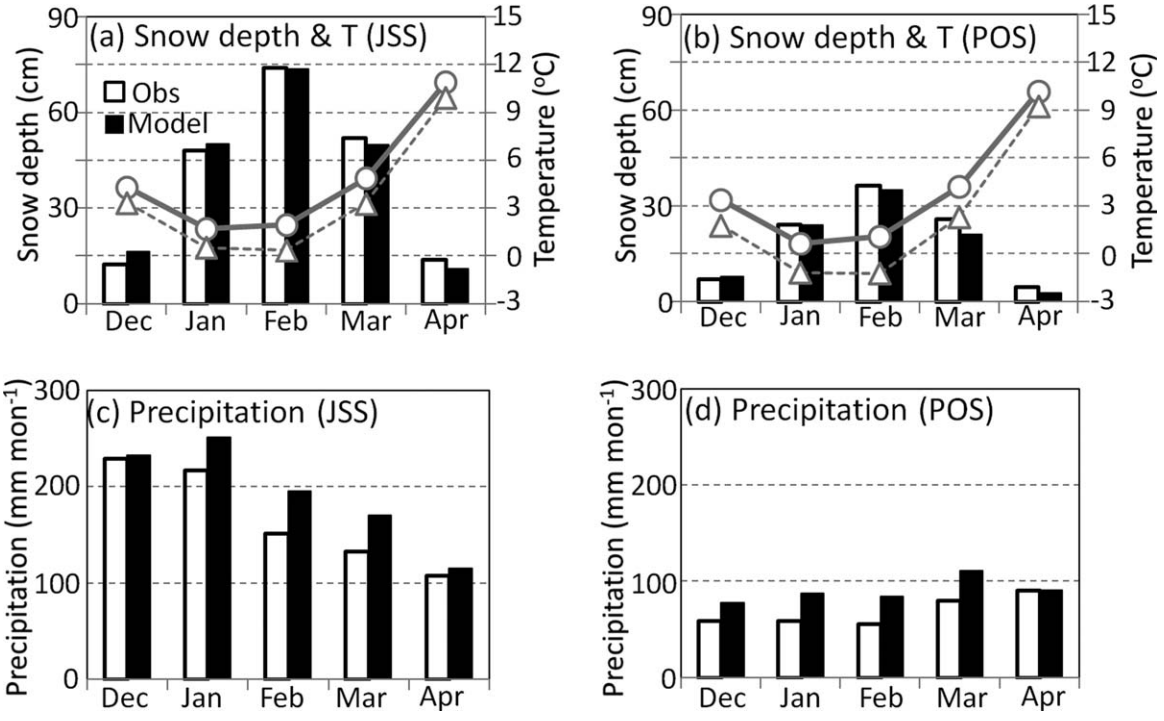

Figure 5. (a and b) Seasonal variation of climatology mean snow depth (cm) and (c and d) precipitation (mm month^{-1}) in observation (white) and REAL runs (black) for JSS (Figures 5a and 5c) and POS (Figures 5b and 5d) regions. Solid and broken lines indicate observed and simulated surface air temperature, respectively.

improved from the JRA-25 by the dynamical downscaling (Figure 7a). The correlation for spatial pattern is higher in the REAL run than that in the JRA-25, which is commonly seen in December–April. In particular, the correlation for downscaled precipitation during December–February is approximately 0.9. The simulated monthly precipitation in JSS region also has a high correlation (>0.8) during December–February (Figure 7b). The precipitation in December and January tends to have low standard deviation. These results indicate the REAL runs well capture the spatial distribution of winter precipitation in Japan.

[14] Despite overestimating the wintertime precipitation and underestimating the temperature, the REAL runs well reproduced the interannual and seasonal variations of precipitation in JSS and JOS regions. Considering the fact that the observations tend to underestimate the actual precipitation, the WRF experiment has the acceptable performance for the purpose of this study.

3.2. Sensitivity of Precipitation to the SST Variability

[15] Figure 8 shows the monthly mean distribution of the DJF precipitation and standard deviation for the interannual

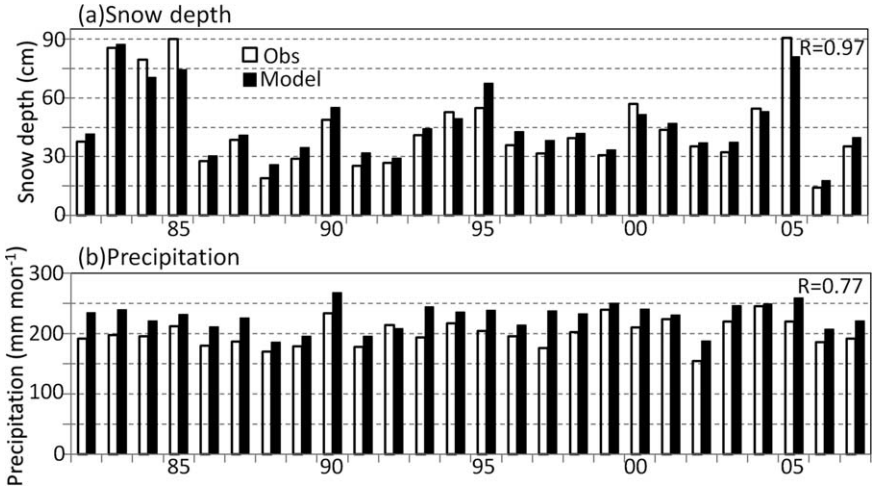

Figure 6. Interannual variation of December-January-February mean (a) snow depth (cm) and (b) precipitation (mm month^{-1}) in observation (white) and REAL runs (black) for JSS region.

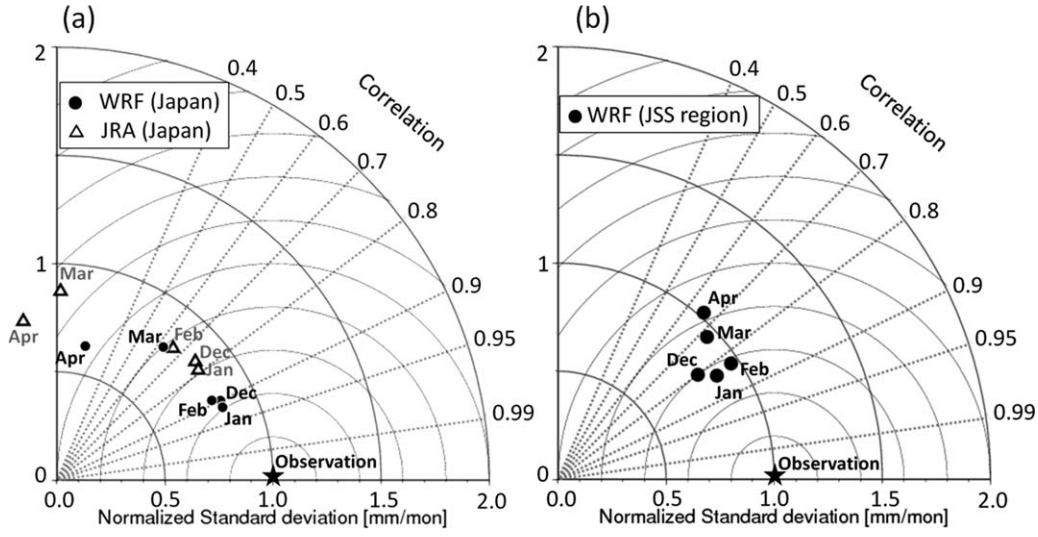

Figure 7. The Taylor diagram of 26 year mean monthly mean precipitation in (a) Japan and (b) JSS region in the REAL runs. The APHRODITE data are used as a reference (star). Open triangles and circles indicate precipitation in JRA-25 and the REAL run, respectively.

variation during 26 winters. It is evident that a large amount of precipitation (>300 mm month^{-1}) falls during December–February along the JSS region, while very less precipitation (<60 mm month^{-1}) is found in the POS region, showing a distinct rain-shadow feature. A weak precipitation zone associated with the rain-shadow extends further over the Pacific Ocean. The DJF precipitation reaches 100 mm month^{-1} over the Pacific Ocean around the area that is a few hundred kilometers eastward of the Japanese islands. The precipitation over the Japan Sea is weak (<30 mm month^{-1}) near the Eurasian continent which gradually increases as the continental air mass undergoes a rapid air-mass transformation over the ocean, eventually exceeding 100 mm month^{-1} along the western coast of the Japanese island. The precipitation pattern in March is completely different from that in DJF, in which a large precipitation zone spreads along the offshore areas of southern and western Japan, corresponding to storm tracks passing around the southwest of Japan in early spring [e.g., *Adachi and Kimura*, 2007]. The narrow precipitation zone becomes ambiguous as storm activities become weak in April.

[16] The ratio of standard deviation of interannual variation of the precipitation to the total precipitation (σ/P) is large over the Eurasian continent where the total precipitation is very little and along southern lateral boundary. The ratio of interannual variation to the total precipitation is small over the oceans. The ratio is constantly high during the cold season with more than 0.5 along the eastern coast of Japan facing the Pacific Ocean indicating that the frequency and track of the extratropical cyclones have a large interannual variability. On the other hand, in the Japan Sea and the JSS region the ratio is small near Japan in correspondence with the large total precipitation. The difference of the standard deviations between REAL and CLIM runs over the Kuroshio extension suggests that the enhancement of the magnitude of interannual variation of the oceanic precipitation is related to the interannual variation of SST. During December–February, the standard deviation of REAL runs over this region increased by 20% compared to that of the CLIM runs. Over the Pacific, the area with enhanced precipitation variability in the REAL runs roughly corresponds to the area with large interannual variation of SST (Figure 3); therefore, SST variability data are essential for accurately predicting the precipitation variability over this area. Despite the large SST variability around the Kuroshio extension, in March, the standard deviation of the REAL runs was similar to that of the CLIM runs. This suggests that the SST variability in March has little impact on the precipitation variability. Whereas in the Japan Sea, the difference of standard deviation between REAL and CLIM runs was mostly below the significant level throughout the winter season despite large SST variability during December–February (Figure 3).

[17] As shown in Figure 8, the standard deviations of the precipitation (σ_{REAL}) are much larger than the impact of SST variability, i.e., a difference between two experiments ($\sigma_{REAL} - \sigma_{CLIM}$), especially over the Japan Sea and over Japanese Island. This suggests that the interannual variations of precipitation over these areas are strongly influenced by the atmospheric variability, such as the winter monsoon as confirmed in Figure 2. Figure 9 shows the standard deviation of DJF mean SST and percentage difference in standard deviation of the precipitation between REAL and CLIM runs. The large variance of SST is located in central Japan Sea and offshore of POS region as those indicated in Figure 3. In the DJF mean pattern, the variance in precipitation is enhanced over the east Japan Sea and the Kuroshio extension corresponding to the downwind areas of the large SST variance although the difference over Japan Sea is not statistically significant. However, Figure 9 indicates the standard deviation of precipitation in the REAL runs is smaller than those in the CLIM runs in north JSS region while it is larger in the neighboring ocean area, showing the opposite tendency between the land and the offshore area. In addition, Figure

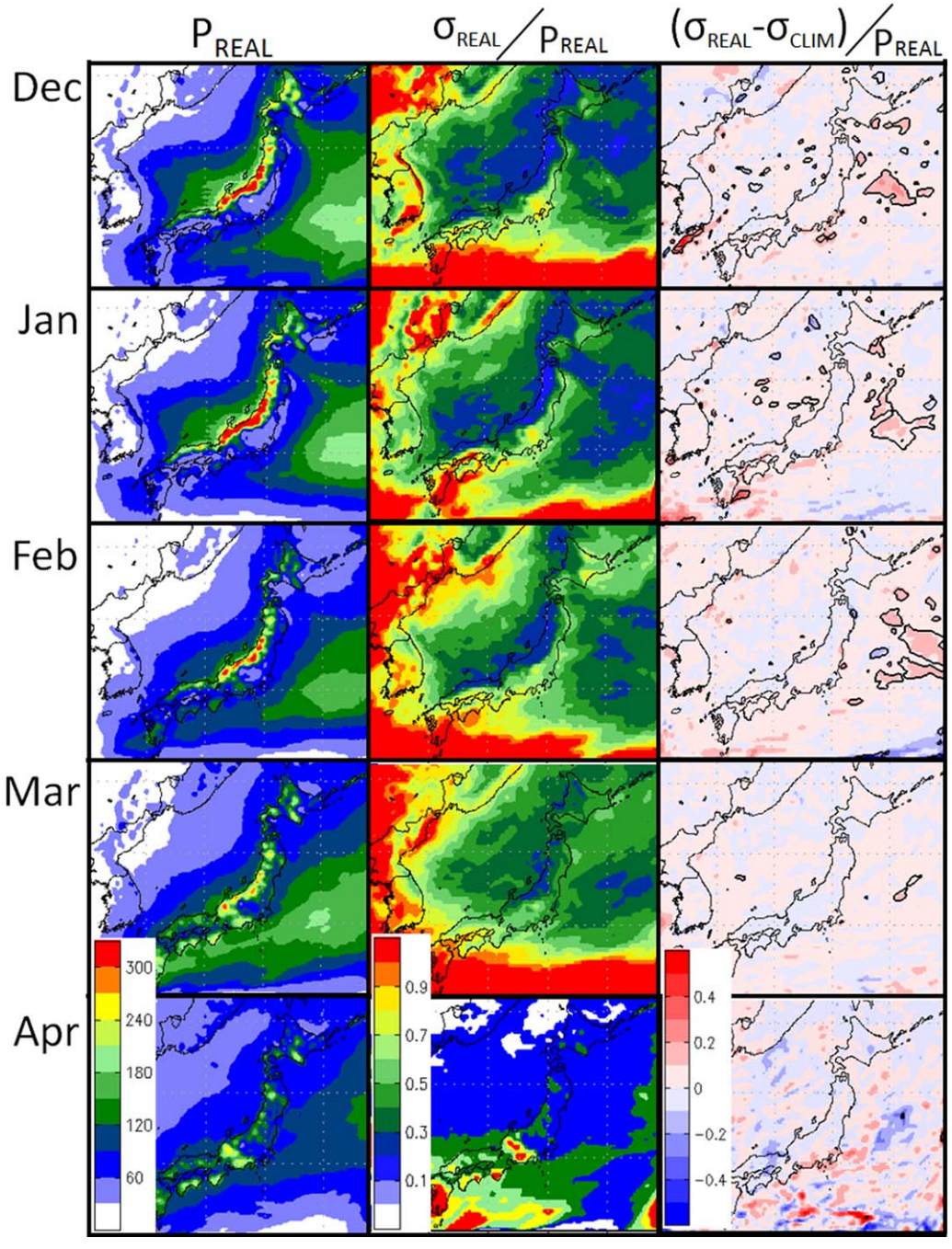

Figure 8. (left) 26 winter mean precipitation (mm month^{-1}) in REAL runs, (middle) their standard deviation for interannual variation divided by the total precipitation, (right) and difference of the standard deviation between REAL and CLIM runs divided by the total precipitation. Solid contour indicates the difference is statistically significant with 90% confidence level.

8 indicates very weak sensitivity of terrestrial precipitation to the SST variability. This would be partly due to large interannual variation of the terrestrial precipitation relative to the impact of the SST's interannual variation. In north JSS region, the large decrease of standard deviation of precipitation in January (no figure) and DJF mean (Figure 9) is located in mountain area. Therefore, mesoscale orographic effect and a choice of microphysics and cumulus schemes are perhaps responsible for the different sensitivities between land and ocean. There is a need for ensemble simulations using different physics schemes in the future studies.

[18] To evaluate the sensitivity of SST for modulating the terrestrial precipitation variability, further analysis was conducted for the JSS region. A detailed precipitation response to the SST forcing can be analyzed using the precipitation difference ($P_{REAL} - P_{CLIM}$) because REAL and CLIM runs are identical except for the forcing SST data

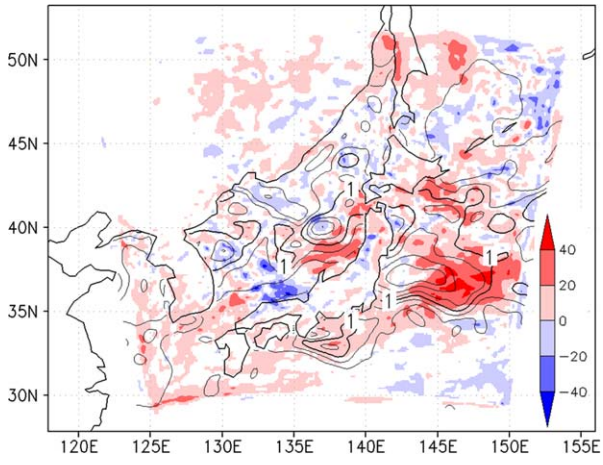

Figure 9. The standard deviation of DJF mean SST (contour: K) and percentage difference in standard deviation of precipitation between REAL and CLIM runs (shade: %). Contour interval is 0.2.

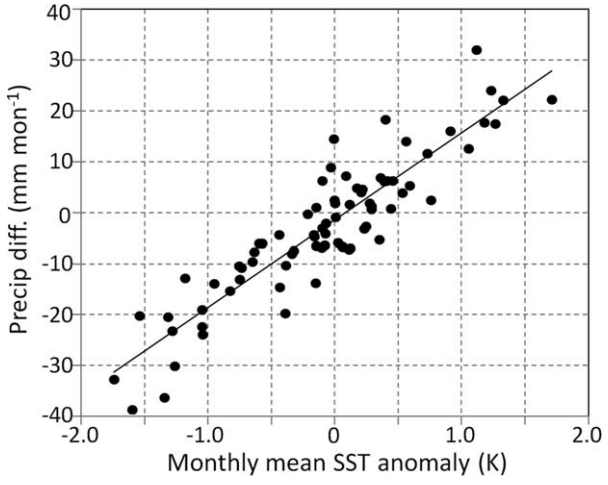

Figure 11. Scatter plot of monthly mean SST anomaly (K) during December–February over area-A (see Fig. 10) and monthly mean precipitation difference (mm month^{-1}) between REAL and CLIM runs in JSS region.

set. Figure 10 illustrates the spatial distribution of the correlation coefficient between the DJF-mean SST anomaly and the DJF precipitation difference between the REAL and CLIM runs ($P_{REAL} - P_{CLIM}$) in the JSS region. The precipitation difference in the JSS region exhibits statistically significant correlation to the SST in the Japan Sea. The highest correlation (>0.8) was found around the offshore areas to the west and northwest of the JSS region. This suggests that SST anomaly in the Japan Sea tends to modify the amount of precipitation in JSS region. This tendency agrees with earlier finding by *Iizuka* [2010], which revealed the influence of narrow high-SST regions on precipitation processes around Japan.

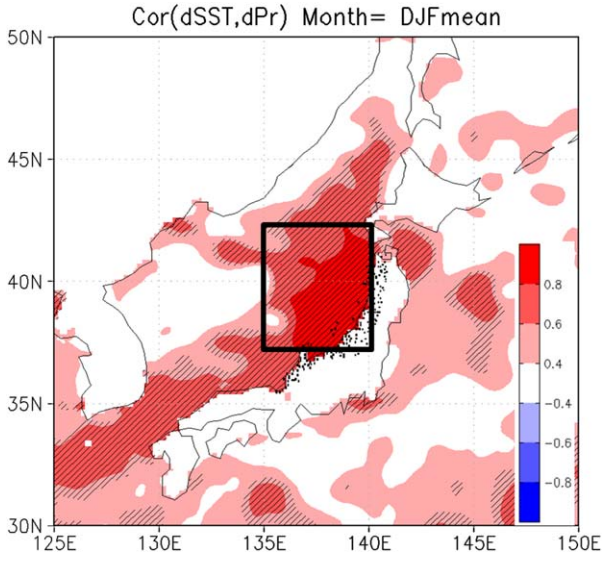

Figure 10. Distribution of correlation coefficient between DJF-mean SST anomaly and DJF precipitation difference between REAL and CLIM runs in JSS region. Solid rectangle shows the area-A (135°E–140°E, 37.5°N–42.5°N) used in Figures 11 and 12. Meteorological stations in JSS region is shown with dots. Hatched area indicates statistically significant correlation with 99% confidence level.

[19] A similar relationship between the DJF means of SST and terrestrial precipitation in JSS exists for the monthly mean precipitation. Figure 11 illustrates the scatter plot for the area-averaged monthly mean SST anomaly at 135°E–140°E, 37.5°N–42.5°N (hereafter, area-A shown in the box in Figure 10), and the precipitation difference ($P_{REAL} - P_{CLIM}$) in the JSS region. The correlations are 0.91 for either December, January, or February. It is obvious that the terrestrial precipitation in JSS is modulated by the SST anomaly because the experimental settings in REAL and CLIM runs are same except for SST. A regression line in Figure 11 indicates that the terrestrial precipitation in JSS region increased by a rate of approximately 16 mm month^{-1} as 1 K SST rise in area-A although the increment is much smaller than the mean precipitation in each month (Figure 8). Despite with rough estimation using model simulations, ratio of the increment relative to the DJF mean precipitation in the REAL run (226.7 mm month^{-1}) is approximately 7%, well corresponding to the Clausius-Clapeyron relationship. From Figure 11, the error/uncertainty in the terrestrial precipitation is estimated to be approximately 10–20 mm month^{-1} corresponding to the 1 K SST error/uncertainty in area-A. Furthermore, the precipitation-SST relationship seems to have little dependency on the year/month. We also confirmed that the $P_{REAL} - P_{CLIM}$ and SST relationship is very similar even if linear trend of SST over the area-A is removed from the scatter plot (not shown). Since the SST variation in the studied period would involve a part of multidecadal variation, the removal of linear trend suggests the precipitation change is not solely due to the decadal variability.

[20] The physical processes that control the SST-precipitation relationship are investigated by composite analysis for the years with warm/cold SST anomalies. Figure 12 shows the interannual variation of the DJF-mean SST anomaly averaged over area-A. The SST was approximately 1 K lower in the 1980s than the climatology, while

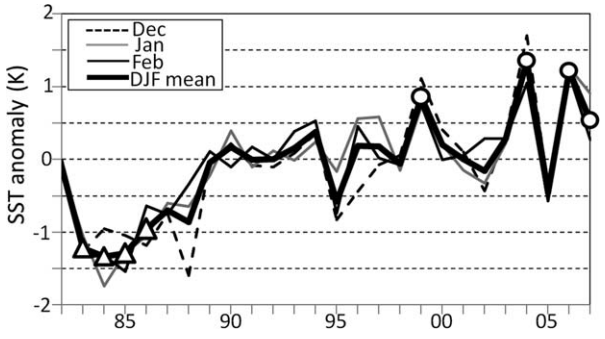

Figure 12. Interannual variation of SST anomaly over area-A (K). Open circles and triangles represent high- and low-SST years in which SST anomalies are larger than +1 or −1 standard deviation, respectively.

it was higher in the 2000s showing an increasing trend during the 1982/1983–2007/2008 although the amplitude of the interannual variation was large. The increasing trends for the individual winter months were very similar to the DJF mean trend. Here, high-SST years and low-SST years are defined when the amplitude of the interannual variation of SST exceeds 1 standard deviation; the winters of 1999/2000, 2004/2005, 2006/2007, and 2007/2008 were selected as the high-SST years and the winters of 1983/1984, 1984/1985, 1985/1986, and 1986/1987 were selected as the low-SST years.

[21] Hereafter, the composite of the anomalous atmospheric patterns between REAL and CLIM is compared to understand the physical processes causing the precipitation change in the JSS region. Since the composite for the low-SST years possesses an almost reverse structure compared to that for the high-SST years, we only show the results for the high-SST years for simplicity. The DJF mean differences between REAL and CLIM for the high-SST years are shown in Figure 13. In the high-SST years, the SST anomaly around the offshore area of the northern JJS region was 2 K higher than the climatology (Figure 13a). The sensible heat flux in the Japan Sea was also larger in the high-SST

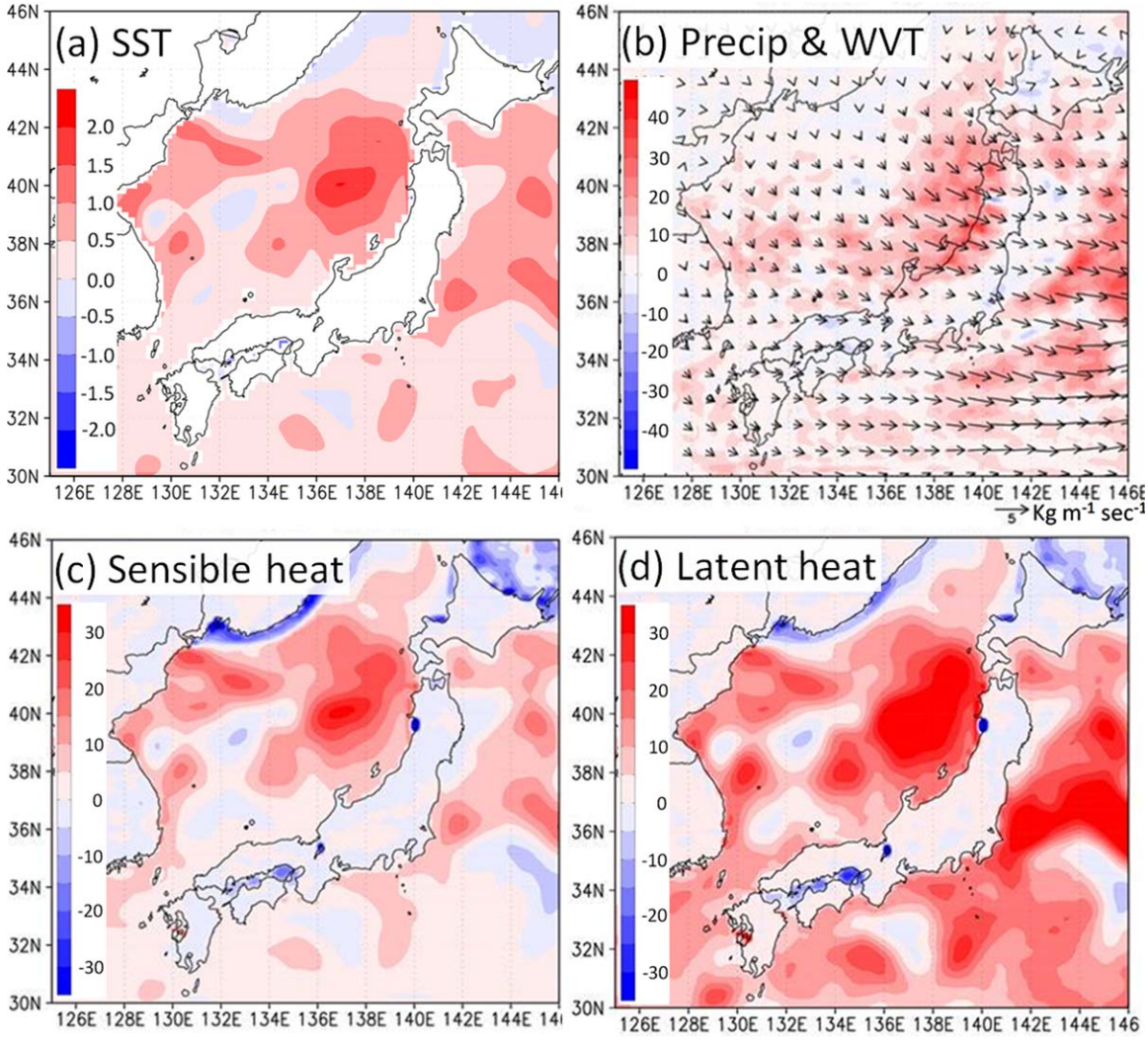

Figure 13. (a) DJF mean SST anomaly (K) for high-SST years. Differences in (b) DJF mean precipitation (mm month^{-1}) and vertically integrated moisture flux (vectors; kg m^{-1} sec^{-1}), (c) sensible heat flux (W m^{-2}), and (d) latent heat flux (W m^{-2}) between REAL and CLIM for high-SST years.

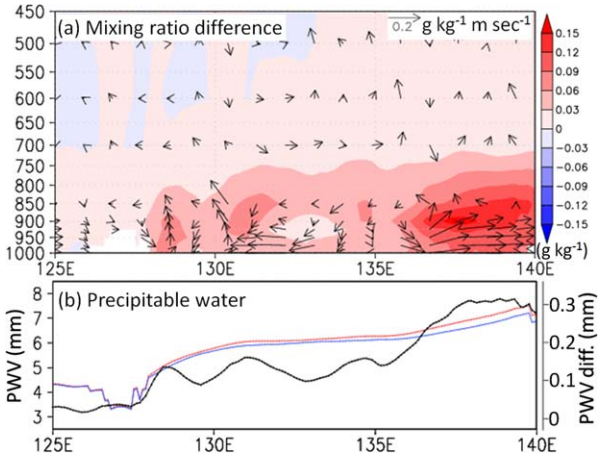

Figure 14. (a) Vertical cross section of the differences in vapor mixing ratio (g kg^{-1}) and wind vector along 39°N. Vertical component of the vector is multiplied by a factor of 50. (b) The precipitable water vapor in the REAL (red) and CLIM (blue) runs and their difference (black).

years by more than 20 W m^{-2} in comparison to the climatology (Figure 13c), probably because of the larger air-sea temperature difference and stronger surface wind in the REAL runs than those in the CLIM runs. The latent heat flux from the Japan Sea increased significantly in accordance with the high SST around area-A (Figure 13d). The moisture flux in the north Japan Sea is intensified over and downwind of the warm SST anomaly because of the increased latent heat flux, which enables more moisture transport toward the JSS regions resulting in the enhanced precipitation in the REAL runs (Figure 13b). A remarkable enhancement of latent heat flux over the Japan Sea and the Pacific Ocean confirms the significant impact of SST on the stronger air-mass transformation in the high-SST years. Figure 13 shows that the increase of the latent heat flux is larger than that of the sensible heat flux. As mentioned in Section 1, the air-mass transformation is strongly affected by the air-sea temperature difference. In this regard, higher SST leads to a higher vapor mixing ratio in the atmosphere at the surface level; this strengthens the vertical gradient of the vapor mixing ratio, resulting in stronger latent heat flux from the surface.

[22] The vertical cross section of the DJF-mean specific humidity for the high-SST years along 39°N is shown in Figure 14. The total moisture content in the lower troposphere slightly increases in the REAL runs because of the increased latent heat flux. The precipitable water vapor is enhanced in REAL runs, especially around area-A. An increase of sensible heat flux also contributes to larger precipitable water vapor values by pushing up the boundary layer height in the REAL runs (not shown). In addition, since increased sensible heat flux promotes active vertical momentum exchange [*Nonaka and Xie*, 2003], the surface wind speed accelerates in the REAL runs around 136–140°E, inducing a further enhancement of surface fluxes. In the high-SST years, both the increased precipitable water vapor and the wind speed in the REAL runs contributed to the increased moisture flux toward Japan that caused more terrestrial precipitation along the central mountains.

[23] We confirmed that the interannual variation of SST enhances the interannual variability of the precipitation around Kuroshio extension in the Pacific Ocean. For the Japan Sea, warmer SST tends to increase terrestrial precipitation along the upwind side of the central mountains in Japan without affecting the magnitude of interannual variability. The precipitation response in JSS region to the SST anomaly in the Japan Sea was robust regardless of the year selected (Figure 11). We examine the relationship between SST trend and precipitation trend in Japan in the following section.

4. SST and Precipitation Trends

[24] The composite analysis for the high-SST years denotes that the terrestrial precipitation is likely to increase with SST warming. Furthermore, Figure 12 demonstrates that SST has an increasing trend around area-A from the winter of 1982/1983 to that of 2007/2008. This section investigates how the long-term precipitation trend is associated with the SST trend.

[25] Figure 15 shows the linear trend of the DJF-mean SST from the winter of 1982/1983 to that of 2007/2008. Although the analyzed period includes a part of the decadal variation, the SST in the northern Japan Sea experienced a marked warming of more than 1 K decade^{-1}, especially around area-A. The statistical analysis by *Matsumura and Xie* [1998] suggested that the SST anomaly in the north Japan Sea around 135–140°E and 40–42.5°N is due to the ocean variability. The SST warming is also observed around the Kuroshio extension during the analysis period. Figure 16 illustrates the DJF-mean precipitation trend from the winter of 1982/1983 to that of 2007/2008 computed using the APHRODITE data set. The observed precipitation indicates an increasing trend in the northern part of the Japanese Islands during the analyzed period and was

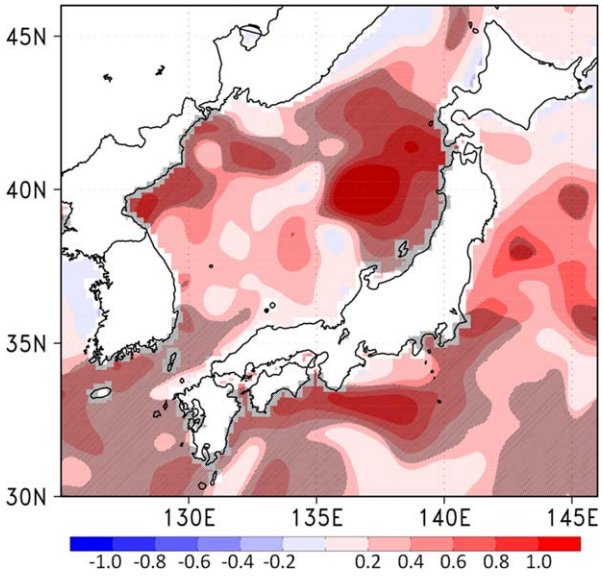

Figure 15. Linear trend of DJF-mean SST (K decade^{-1}) from the winter of 1982/1983 to that of 2007/2008. Dark shadings indicate trends are statistically significant with 95% confidence level.

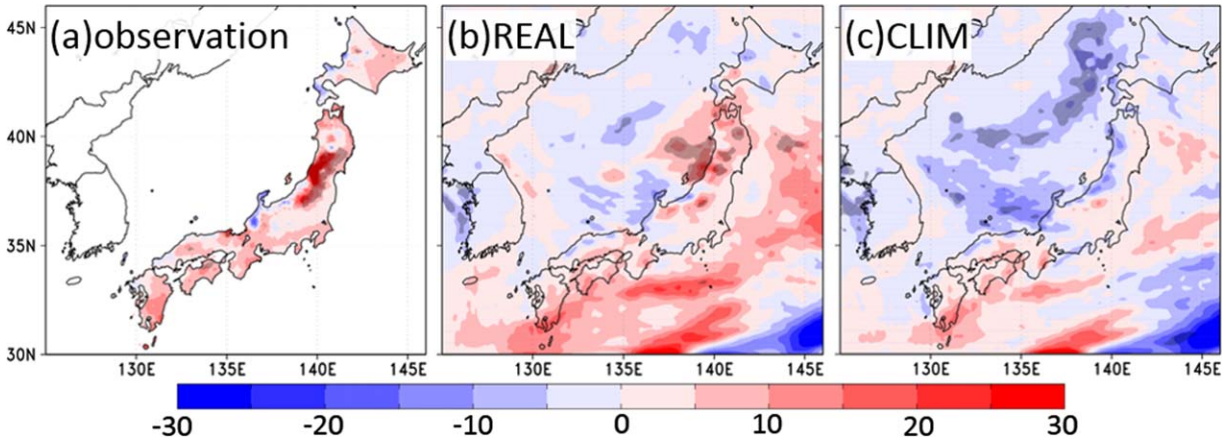

Figure 16. Linear trends of the DJF mean precipitation (mm month^{-1} decade^{-1}) from the winter of 1982/1983 to that of 2007/2008. (a) Observation, (b) REAL runs, and (c) CLIM runs. Hatching indicate trends are statistically significant with 95% confidence level.

statistically significant with 95% confidence level by the Student's *t* test (Figure 16a). The precipitation trends are also significant in the southern Japan. A decreasing trend is locally distributed around the southern JSS region though this is not statistically significant. The precipitation trends in the REAL runs produced a similar increasing trend in many regions in Japan, though not statistically significant. Moreover, the REAL runs simulated the weak precipitation decrease around the southern JSS region (not statistically significant). Both observation and REAL runs showed the largest and statistically significant increase in DJF mean precipitation around the northern JSS region. This indicates that WRF was able to simulate the long-term trend of wintertime precipitation around Japan to some extent although there is a noticeable bias in the climatologically mean state (Figures 5 and 6). The simulated precipitation change around the Japan Sea is similar to the coarse resolution regional model simulation by *Hong and Yhang* [2010] which showed precipitation difference between 1999–2007 and 1979–1987 with 50 km mesh model. The current study is the first one that demonstrates long-term terrestrial precipitation trend in north Japan during winter monsoon by means of regional atmospheric modeling.

[26] The precipitation trends in the CLIM runs were very different from those in the REAL runs. The increasing trends evident in the observations and the REAL runs were rather weakened in the CLIM runs over almost the entire domain, and some of the areas, such as the JSS region, even tend to show a decreasing trend in the CLIM runs (Figure 16c). The remarkable difference in the terrestrial precipitation trend around the JSS region strongly suggests that SST warming has a crucial role in the precipitation trends in northern Japan. In the CLIM runs, a decreasing trend in the precipitation over the JSS region seems to be connected with a broad decreasing feature over the southern Japan Sea. Since there is no interannual variation of SST in the CLIM runs, the decrease in precipitation is solely induced by the long-term variations in atmospheric forcing. Indeed, earlier studies have pointed out a recent weakening of the winter monsoon after the late 1980s [e.g., *Wang et al*., 2009]. *Takano et al*. [2008] suggested that a weaker winter monsoon leads to a weaker air-mass modification over the Japan Sea; therefore, the precipitation decrease in the CLIM run is likely attributed to the recent weakening of heat and moisture flux due to the winter monsoon change. Furthermore, Figures 16b and 16c suggests that the precipitation trends over the oceans are more strongly affected by the recent SST warming around Japan.

[27] A possible impact of SST warming in Japan Sea on the terrestrial precipitation in Japan is summarized in Figure 17. The two experiments clarified that the SST trend in the Japan Sea during the 1980s–2000s was sufficiently large to alter the precipitation trends in Japan. As mentioned above, the weak (or warmer) winter monsoons tend to reduce the precipitation in the JSS region (as inferred from Figure 16c), whereas the warmer SST tends to enhance precipitation by increasing the horizontal moisture advection toward Japan (Figure 13b); therefore, indicating the contrary effects of winter monsoon and SST. The precipitation has increased in the northern JSS region probably because of the stronger influence of the warming SST. Meanwhile, the southern JSS region suffered from a stronger influence of the weakened winter monsoon, resulting in a declining trend in the REAL runs. The observed decrease in the southern JSS region seems to originate from a weakened low-level convergence in the southern Japan Sea, the so-called Japan Sea polar air mass convergence zone (JPCZ). The JPCZ is maintained by the low-level convergence generated downstream of the north Korean mountains, bringing heavy snowfall to Japan [*Asai*, 1988; *Yoshizaki et al*., 2004]. The CLIM runs suggested that the precipitation along the JPCZ had weakened dramatically since the 1980s because of the changes in atmospheric forcing.

[28] Besides precipitation decrease along JPCZ, another line-shaped decreasing trend is evident in the north Japan Sea which is recognizable in the REAL runs (Figure 16b) but with more pronounced in the CLIM runs (Figure 16c). The area of strongest decreasing trend is oriented with southwest-northeast direction that is collocated with the major SST front in north Japan Sea in winter (Figure 3). In the REAL runs, large interannual variation of SST near the front weakens the atmosphere-induced decreasing trend in this area. The prominent decreasing trend in the CLIM runs

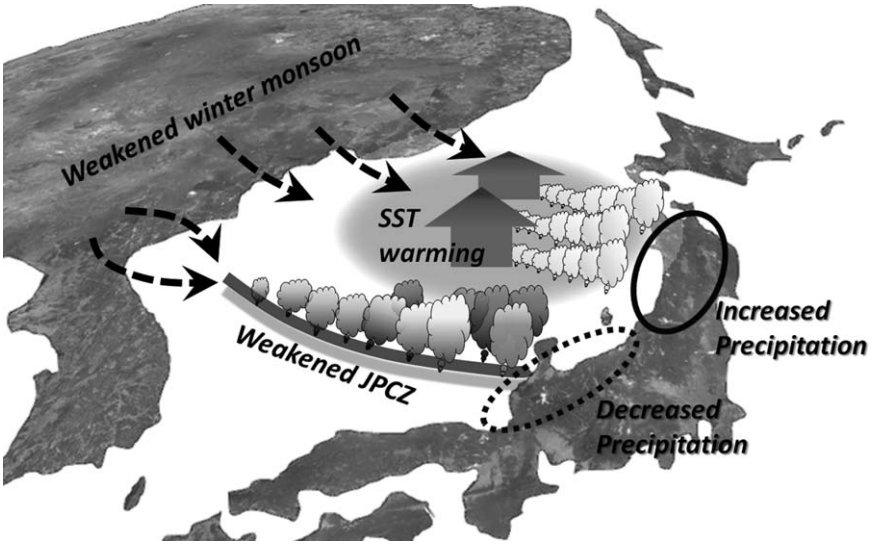

Figure 17. Schematic diagram showing the impact of SST warming on the precipitation change in JSS regions in Japan.

indicates the weakening of the vertical instability due to the stronger warming in the Eurasian continent than the Japan Sea. The air-mass transformation tends to be more prominent near the warm side of the SST front. The weaker (or warmer) winter monsoon is expected to cause a slowdown of the air-mass transformation, and hence, the location of rapid condensation is likely to shift downwind with a parallel structure to the SST front. Another possibility for such a strong trend in CLIM runs is that the experiment using the atmospheric model would estimate stronger impact of SST forcing than the experiment using the atmosphere-ocean coupled model. In the actual atmosphere-ocean coupled system, the cold winter monsoon will cool the SST from early to late winter, which will work to reduce atmosphere-ocean temperature difference. However, the atmosphere-only experiment does not have this negative feedback process, resulting in strong sensitivity to the given SST forcing.

5. Discussion

[29] In this section, the role of SST in precipitation over the Pacific Ocean and adjacent land areas in Japan will be first addressed. As mentioned in section 1, the local climate in the POS region is characterized by dry and clear weather owing to the rain-shadow effect of the central mountains (Figure 2). Winter precipitation in the POS region is mainly brought in by the extratropical cyclones passing across Japan or passing near the southeastern coastal areas. Since the storms become active in early winter (December) and early spring (from March to April) [e.g., *Adachi and Kimura*, 2007], heavy precipitation occasionally occurs during these months. The heavy snowfall and rapid temperature drop associated with the cyclone passage causes hazardous weather that can affect many regions in central and northern Japan [e.g., *Hirota et al*., 2006].

[30] The precipitation tends to have a large variance around the storm track (Figure 8) since the amount of precipitation differs largely from one storm event to the other. Observations and modeling studies have shown that SST forcing alters storm activities around the Kuroshio extension [e.g., *Nonaka and Xie*, 2003; *Tokinaga et al*., 2006; *Taguchi et al*., 2009; *Koseki and Watanabe*, 2010]. The DJF precipitation increased more rapidly in the REAL runs compared to that in the CLIM runs over the Pacific Ocean (Figure 16), which suggests that the SST warming has a positive influence on the precipitation over the Pacific Ocean, and is consistent with the data analysis for the extratropical cyclone development by *Iwao et al*. [2012]. Furthermore, it is interesting to note that the precipitation in CLIM runs also possesses a weak increasing trend around southeastern Japan and regions facing the Pacific Ocean. A plausible explanation for this is that the characteristics of the storms have changed, bringing more precipitation around Japan, for example, changes in frequency, development, or intensity [e.g., *Iwao et al*., 2012], and their tracks have shifted closer to the Japanese islands [*Nakamura et al*., 2012]. Since the performance of the REAL runs for cyclone-derived precipitation in the POS region was not as good as that in the JSS region where larger fraction of precipitation is brought by winter monsoon. In order to realistically simulate cyclone's track and intensity, high-resolution SST data set would be helpful [*Iizuka*, 2010]. Recently, a space-borne high-resolution SST data set revealed that the small structures in the SST distribution played a role in modulating the near-surface wind over the oceans [*Chelton et al*., 2004]. Therefore, the use of high-resolution SST data sets, such as those summarized in *Martin et al*. [2012], is a promising approach to improve the air-sea interaction in the model, and hence, we will be able to discuss a detailed effect of SST warming and precipitation change proposed in this study.

[31] Since snowfall events in northern Japan occur at temperature ranges between snow and rain (i.e., near freezing temperature), the snowfall in Japan is highly sensitive to any temperature rise that is expected to happen under global warming. The available future projections based on dynamical downscaling experiments suggested that the

snow depth in northern Japan is showing a decreasing trend [*Hara et al*., 2008; *JMA*, 2008; *Matsumura and Sato*, 2011] that may cause significant changes in the availability of water resources in this region and in river discharges [*Ma et al*., 2010]. However, according to the earlier studies, the downscaled future projection may contain uncertainties associated with the treatment of SST data because future SST may differ depending on the behavior of the ocean currents [e.g., *Choi et al*., 2002]; this would make the mesoscale SST distribution quite different from that used in the earlier downscaling studies. The sensitivity test for terrestrial precipitation in this study was useful to verify the uncertainties in precipitation derived from the SST uncertainty. The decreasing trend in precipitation around the southern JSS region is an interesting topic to study in relation to the possible changes in the JPCZ. Sensitivity experiment such as the CLIM runs are a useful approach that switches off a certain process to evaluate its importance in the climate system. The weakening of winter monsoon is a common feature in GCMs under the warming climate [*Hori and Ueda*, 2006; *Intergovernmental Panel on Climate Change*, 2007]. This study suggests that reliable SST prediction is essential to accurately evaluate precipitation trends in northern Japan.

[32] A critical issue that needs to be solved in the future study is the influence of SST for changing the snow depth trends. We compared the long-term trends in mean snow depth between the two experiments. Both experiments show snow depth decrease in low altitude and increase in mountain areas except for the localized increase in north JSS region in the REAL runs (no figure) where precipitation has been increased in Figure 16b. This perhaps comes from the strong sensitivity of snow to the air temperature during snowfall and melting which is probably related to the cloud microphysics and land surface schemes. *Kawase et al*. [2012] suggested that the change in snow depth that occurred during the 1980s and 1990s around the southern JSS region was caused by the changes in mean atmosphere and ocean structure including their temperature changes. Further studies are needed to clarify the influence of the rising atmospheric temperature by modulating the snow/rainfall rate, maybe with a cloud-resolving model, which will help evaluating the impact of climate change on water resources in the snowy regions.

6. Conclusions

[33] Large amounts of snowfall occurs over northern Japan as the westerly winter monsoon carries abundant moisture supplied from the Japan Sea and is forced to ascend along the central mountains of the Japanese Islands. To investigate the role of SST in modulating the terrestrial precipitation in Japan, numerical experiments using the WRF model were conducted with a grid size of 20 km. Two numerical experiments were conducted for the 26 winters of 1982/1983–2007/2008; one with a realistic daily SST distribution obtained from OISST (the REAL runs) and another using climatology SST data with a mean seasonal variation (the CLIM runs).

[34] In the REAL runs, WRF successfully simulated the seasonal and interannual variation of the mean snow depth in the JSS region although the precipitation seemed larger than the observations. The REAL runs showed larger standard deviation for the interannual variation of the precipitation over the Pacific Ocean during December–February relative to those in the CLIM runs, suggesting that the SST variability enhances the precipitation variability around the Kuroshio extension. The precipitation variability is locally intensified in the area over and the downwind of high SST variability.

[35] The analysis for the years with high SST in the Japan Sea indicated that the terrestrial precipitation in the JSS region was highly sensitive to the offshore SST anomaly around the central to eastern parts of the Japan Sea although the magnitude of interannual variation was not significantly affected. The warmer SST tended to increase the sensible and latent heat flux and to accelerate the low-level wind more than the climatology SST, resulting in larger moisture flux toward Japan. Since the SST in the Japan Sea exhibited a warming trend during the 1980s to 2000s, we investigated the effect of the long-term SST variation on the terrestrial precipitation trend in Japan. The REAL runs produced significant increasing trend in the northern JSS region and a weak decreasing trend in the southern JSS region, which were similar to those of the observations. In contrast, the CLIM runs showed a weak decreasing trend over almost the entire JSS region, consistently with the weakening of the winter monsoon. This suggests that although the atmospheric forcing reduces the precipitation in the JSS region, the precipitation has increased, especially around the northern JSS region, because of the warmer SST during the 2000s. Therefore, we conclude that the long-term SST trend is an essential driving force for the precipitation trend in Japan and the adjacent oceans where SST has significant increasing/decreasing trends. The CLIM runs further indicate that the weakening of the JPCZ is likely responsible for the localized precipitation decrease around the southern JSS region. The precipitation in southern Japan facing the Pacific Ocean indicated increasing trend even without the SST's warming trend. This suggests that changes in the extratropical cyclone characteristics, such as changes in storm intensity and shifts of the storm track axis, are also an important factor affecting the precipitation trends around the Kuroshio extension.

[36] **Acknowledgments.** The authors appreciate the anonymous reviewers for their useful comments. The suggestions raised by Professor Shang-Ping Xie helped improving the manuscript. This study was supported by the grant-in-aid for Scientific Research on Innovative Areas (25106701) funded by JSPS, the Environment Research and Technology Development Fund (S-8-1(2)) of the Ministry of the Environment, Japan, and the Research Program on Climate Change Adaptation (RECCA), and the Green Network of Excellence (GRENE) Program in the Arctic Climate Change Research Project of the Ministry of Education, Culture, Sports, Science, and Technology, Japan. The APHRODITE data set was obtained from the project web site (http://www.chikyu.ac.jp/precip/).

References

Adachi, S., and F. Kimura (2007), A 36-year climatology of surface cyclogenesis in east Asia using high-resolution reanalysis data, *SOLA*, *3*, 113–116, doi:10.2151/sola.2007–029.

Asai, T. (1988), Mesoscale features of heavy snowfalls in Japan Sea coastal regions of Japan. (in Japanese), *Tenki*, *35*, 156–161.

Chelton, D. B., M. G. Schlax, M. H. Freilich, and R. F. Milliff (2004), Satellite measurements reveal persistent small-scale features in ocean winds. *Science*, *303*, 978–983.

Chen, F., and J. Dudhia (2001), Coupling an advanced land surface/hydrology model with the Penn State/NCAR MM5 modeling system. Part I: Model description and implementation, *Mon. Weather Rev.*, *129*, 569–585.

Choi, B.-H., D.-H. Kim, and J.-W. Kim (2002), Regional responses of climate in the Northwestern Pacific Ocean to gradual global warming for a CO2 quadrupling, *J. Meteorol. Soc. Jpn.*, *80*, 1427–1442.

Ding, Y. (1994), *Monsoons Over China*, 420 pp., Kluwer Acad., Netherlands.

Dudhia, J. (1989), Numerical study of convection observed during the winter monsoon experiment using a mesoscale two-dimensional model, *J. Atmos. Sci.*, *46*, 3077–3107.

Grell, G. A., and D. Devenyi (2002), A generalized approach to parameterizing convection combining ensemble and data assimilation techniques, *Geophys. Res. Lett.*, *29*(14), 1693, doi:10.1029/2002GL015311.

Gutmann, E. D., R. M. Rasmussen, C. Liu, K. Ikeda, D. J. Gochis, M. P. Clark, J. Dudhia, and G. Thompson (2012), A comparison of statistical and dynamical downscaling of winter precipitation over complex terrain, *J. Clim.*, *25*, 262–281.

Hara, M., T. Yoshikane, H. Kawase, and F. Kimura (2008), Estimation of the impact of global warming on snow depth in Japan by the Pseudo-Global-Warming method, *Hydro. Res. Lett.*, *2*, 61–64, doi:10.3178/hrl.2.61.

Hirose, N., and K. Fukudome (2006), Monitoring the Tsushima warm current improves seasonal prediction of the regional snowfall, *SOLA*, *2*, 61–63, doi:10.2151/sola.2006–016.

Hirota, T., Y. Iwata, M. Hayashi, S. Suzuki, T. Hamasaki, R. Sameshima, and I. Takayabu (2006), Decreasing soil-frost depth and its relation to climate change in Tokachi, Hokkaido, Japan, *J. Meteorol. Soc. Jpn.*, *84*, 821–833.

Hong, S.-Y., and J.-O. J. Lim (2006), The WRF single-moment 6-Class microphysics scheme (WSM6), *J. Korean Meteorol. Soc.*, *42*, 129–151.

Hong, S.-Y., and Y.-B. Yhang (2010), Implications of a decadal climate shift over East Asia in winter: A modeling study, *J. Clim.*, *23*, 4989–5001.

Hong, S.-Y., J. Dudhia, and S.-H. Chen (2004), A revised approach to ice microphysical processes for the bulk parameterization of clouds and precipitation, *Mon. Weather Rev.*, *132*, 103–120.

Hori, M. E., and H. Ueda (2006), Impact of global warming on the East Asian winter monsoon as revealed by nine coupled atmosphere-ocean GCMs, *Geophys. Res. Lett.*, *33*, L03713, doi:10.1029/2005GL024961.

Iizuka, S. (2010), Simulations of wintertime precipitation in the vicinity of Japan: Sensitivity to fine-scale distributions of sea surface temperature, *J. Geophys. Res.*, *115*, D10107, doi:10.1029/2009JD012576.

Intergovernmental Panel on Climate Change (2007), Climate Change 2007: The Physical Science Basis, in *Contribution of Working Group I to the Fourth Assessment Report of the IPCC*, edited by S. Solomon et al., 996 pp., Cambridge Univ. Press, Cambridge, U. K.

Iwao, K., M. Inatsu, and M. Kimoto (2012), recent changes in explosively developing extratropical cyclones over the winter northwestern pacific, *J. Clim.*, *25*, 7282–7296.

JMA (2008), *Global Warming Projection*, vol. 7, Tokyo, (in Japanese). [Available at http://www.data.kishou.go.jp/climate/cpdinfo/GWP/Vol7/pdf/synthesis.pdf.]

Kamiguchi, K., O. Arakawa, A. Kitoh, A. Yatagai, A. Hamada, and N. Yasutomi (2010), Development of APHRO_JP, the first Japanese high-resolution daily precipitation product for more than 100 years, *Hydro. Res. Lett.*, *4*, 60–64.

Kawase, H., T. Yoshikane, M. Hara, M. Fujita, N. N. Ishizaki, F. Kimura, and H. Hatsushika (2012), Downscaling of snow cover changes in the late 20th century using a past climate simulation method over central Japan, *SOLA*, *8*, 61–64.

Koseki, S., and M. Watanabe (2010), Atmospheric boundary layer response to mesoscale SST anomalies in the Kuroshio extension, *J. Clim.*, *23*, 2492–2507.

Ma, X., T. Yoshikane, M. Hara, Y. Wakazuki, H. Takahashi, and F. Kimura (2010), Hydrological response to future climate change in the Agano River basin, *Japan. Hydrol. Res. Lett.*, *4*, 25–29.

Manabe, S. (1957), On the modification of air-mass over the Japan Sea when the outburst of cold air predominates, *J. Meteorol. Soc. Jpn.*, *35*, 311–326.

Martin, M. (2012), Group for high resolution sea surface temperature (GHRSST) analysis fields inter-comparisons: Part A GHRSST Multi-Product Ensemble (GMPE), *Deep Sea Res., Part II*, *77–80*, 21–30, doi:10.1016/j.dsr2.2012.04.013.

Matsumura, S., and T. Sato (2011), Snow/ice and cloud responses to future climate change around Hokkaido, *SOLA*, *7*, 205–208.

Matsumura, S., and S.-P. Xie (1998), Response of temperature and precipitation over Japan and the Japan Sea to variability of winter monsoon, *Tenki*, *45*, 781–791 (in Japanese with English abstract).

Mlawer, E. J., S. J. Taubman, P. D. Brown, M. J. Iacono, and S. A. Clough (1997), Radiative transfer for inhomogeneous atmosphere: RRTM, a validated correlated-k model for the longwave, *J. Geophys. Res.*, *102*(D14), 16,663–16,682.

Nakamura, H., A. Nishina, and S. Minobe (2012), Response of storm tracks to bimodal Kuroshio path states south of Japan, *J. Clim.*, *25*, 7772–7779, doi:10.1175/JCLI-D-12–00326.1.

Nakanishi, M., and H. Niino (2004), An improved Mellor–Yamada level-3 model: Its design and verification, *Boundary Layer Meteorol.*, *112*, 1–31.

Nakanishi, M., and H. Niino (2006), An improved Mellor–Yamada level-3 model: Its numerical stability and application to a regional prediction of advecting fog, *Boundary Layer Meteorol.*, *119*, 397–407.

Ninomiya, K. (1968), Heat and water budget over the Japan Sea and the Japan island in winter season, *J. Meteorol. Soc. Jpn.*, *46*, 342–372.

Nonaka, M., and S.-P. Xie (2003), Covariations of sea surface temperature and wind over the Kuroshio and its extension: Evidence for ocean-to-atmosphere feedback, *J. Clim.*, *16*, 1404–1413.

Onogi K., et al. (2007), The JRA-25 reanalysis, *J. Meteorol. Soc. Jpn.*, *85*, 369–432.

Reynolds, R. W., T. M. Smith, C. Liu, D. B. Chelton, K. S. Casey, and M. G. Schlax (2007), Daily high resolution blended analysis for sea surface temperatures, *J. Clim.*, *20*, 5473–5496, doi:10.1175/2007JCLI1824.1.

Saito, K., M. Murakami, T. Matsuo, and H. Mizuno (1996), Sensitivity experiments on the orographic snowfall over the mountainous region of northern Japan, *J. Meteorol. Soc. Jpn.*, *74*, 797–813.

Sato, T., and Y. Xue (2013), Validating regional climate model's downscaling ability for East Asian summer monsoonal interannual variability, *Clim. Dyn.*, *41*, 2411–2426, doi:10.1007/s00382-012-1616-5.

Skamarock, W. C., J. B. Klemp, J. Dudhia, D. O. Gill., D. M. Barker., M. G. Duda, X.-Y., Huang, W. Wang., and J. G. Powers (2008), A description of the advanced research WRF version 3, NCAR Tech. Note NCAR/TN–475+STR.

Taguchi, B., H. Nakamura, M. Nonaka, and S.-P. Xie (2009), Influences of the Kuroshio/Oyashio extensions on air–sea heat exchanges and storm-track activity as revealed in regional atmospheric model simulations for the 2003/04 cold season, *J. Clim.*, *22*, 6536–6560.

Takano, Y., Y. Tachibana, and K. Iwamoto (2008), Influences of large-scale atmospheric circulation and local sea surface temperature on convective activity over the Sea of Japan in December, *SOLA*, *4*, 113–116.

Taylor, K. E. (2001), Summarizing multiple aspects of model performance in a single diagram, *J. Geophys. Res.*, *106*, 7183–7192, doi:10.1029/2000JD900719.

Tokinaga, H., Y. Tanimoto, M. Nonaka, B. Taguchi, T. Fukamachi, S.-P. Xie, H. Nakamura, T. Watanabe, and I. Yasuda (2006), Atmospheric sounding over the winter Kuroshio extension: Effect of surface stability on atmospheric boundary layer structure, *Geophys. Res. Lett.*, *33*, L04703, doi:10.1029/2005GL025102.

Wang, B. (2006), *The Asian Monsoon*, 787 pp., Springer PRAXIS, U. K.

Wang, L., R. Huang, L. Gu, W. Chen, and L. Kang (2009), Interdecadal variations of the East Asian winter monsoon and their association with quasi-stationary planetary wave activity, *J. Clim.*, *22*, 4860–4872.

Xu, H., M. Xu, S.-P. Xie, and Y. Wang (2011), Deep atmospheric response to the spring Kuroshio over the East China Sea, *J. Clim.*, *24*, 4959–4972.

Yamaguchi, S., S. Nakai, K. Iwamoto, and A. Sato (2009), Influence of anomalous warmer winter on statistics of measured winter precipitation data, *J. Appl. Meteorol. Climatol.*, *48*, 2403–2409.

Yasuda, T., and K. Hanawa (1999), Composite analysis of North Pacific subtropical mode water properties with respect to the strength of the wintertime East Asian monsoon, *J. Oceanogr.*, *55*, 531–541.

Yoshizaki, M., T. Kato, H. Eito, S. Hayashi, and W.-K. Tao (2004), An overview of the field experiment "Winter mesoscale convective systems (MCSs) over the Japan Sea in 2001", and comparisons of cold-air outbreak case (14 January) between analysis and a non-hydrostatic cloud-resolving model, *J. Meteorol. Soc. Jpn.*, *82*, 1365–1387.